4. Dykha, A. V. Distribution of friction tangential stresses in the Courtney-Pratt experiment under Bowden's theory [Text] / A. V. Dykha, A. G. Kuzmenko // Journal of Friction and Wear. – 2016. – Vol. 37, Issue 4. – P. 315–319. doi: 10.3103/s1068366616040061
5. Bulgarevich, S. B. Kinetics of sample wear on four-ball friction-testing machine using lubricants of different consistencies [Text] / S. B. Bulgarevich, M. V. Boiko, K. S. Lebedinskii, D. Yu. Marchenko // Journal of Friction and Wear. – 2014. – Vol. 35, Issue 6. – P. 531–537. doi: 10.3103/s106836661406004x
6. Dykha, A. V. Solution to the problem of contact wear for a four-ball wear-testing scheme [Text] / A. V. Dykha, A. G. Kuzmenko // Journal of Friction and Wear. – 2015. – Vol. 36, Issue 2. – P. 138–143. doi: 10.3103/s1068366615020051
7. Rezaei, A. Adaptive finite element simulation of wear evolution in radial sliding bearings [Text] / A. Rezaei, W. Van Paepegem, P. De Baets, W. Ost, J. Degrieck // Wear. – 2012. – Vol. 296, Issue 1-2. – P. 660–671. doi: 10.1016/j.wear.2012.08.013
8. Dykha, A. Determining the characteristics of viscous friction in the sliding supports using the method of pendulum [Text] / A. Dykha, V. Aulin, O. Makovkin, S. Posonskiy // Eastern-European Journal of Enterprise Technologies. – 2017. – Vol. 3, Issue 7 (87). – P. 4–10. doi: 10.15587/1729-4061.2017.99823
9. Vynar, V. A. Influence of the Stress-strain State on the Wear Resistance of the Surface of 40Kh Steel after Discrete Electromechanical Treatment [Text] / V. A. Vynar, M. O. Dykha // Materials Science. – 2013. – Vol. 49, Issue 3. – P. 375–381. doi: 10.1007/s11003-013-9625-z
10. Kryshtopa, S. Examining the effect of triboelectric phenomena on wear-friction properties of metal-polymeric frictional couples [Text] / S. Kryshtopa, L. Kryshtopa, I. Bogatchuk, I. Prunko, V. Melnyk // Eastern-European Journal of Enterprise Technologies. – 2017. – Vol. 1, Issue 5 (85). – P. 40–45. doi: 10.15587/1729-4061.2017.91615
11. Kindrachuk, M. The friction mechanism between surfaces with regular micro grooves under boundary lubrication [Text] / M. Kindrachuk, O. Radionenko, A. Kryzhanovskyi, V. Marchuk // Aviation. – 2014. – Vol. 18, Issue 2. – P. 64–71. doi: 10.3846/16487788.2014.926642

Розглянуто задачу визначення картини усталеного трифазного режиму руху зернистого заповнення у поперечному перерізі циліндричної камери, що обертається навколо горизонтальної осі. Застосовано аналітико-експериментальний метод дослідження. Визначено положення квазітвердотільної зони невільного падіння і зсувного шару заповнення та розподіл швидкостей у нормальних перерізах потоків. Виявлено залежності характеристик картини руху від параметрів системи. Результати розрахунку картин добре збігаються із експериментальними даними

Ключові слова: зернисте заповнення, обертова камера, трифазний режим руху, картина руху, візуалізація

Рассмотрена задача определения картины установившегося трехфазного режима движения зернистого заполнения в поперечном сечении цилиндрической камеры, вращающейся вокруг горизонтальной оси. Применен аналитико-экспериментальный метод исследования. Определено положение квазитвердотельной зоны несвободного падения и сдвигового слоя заполнения и распределение скоростей в нормальных сечениях потоков. Выявлены зависимости характеристик картины движения от параметров системы. Результаты расчета картин хорошо совпадают с экспериментальными данными

Ключевые слова: зернистое заполнение, вращающаяся камера, трехфазный режим движения, картина движения, визуализация

UDC 621.926.5 : 539.215
DOI: 10.15587/1729-4061.2017.110444

MODELING A FLOW PATTERN OF THE GRANULAR FILL IN THE CROSS SECTION OF A ROTATING CHAMBER

Yu. Naumenko
Doctor of Technical Sciences,
Associate Professor
Department of construction, road, reclamation, agricultural machines and equipment
National University of Water and Environmental Engineering
Soborna str., 11, Rivne, Ukraine, 33028
E-mail: informal9m@i.ua

1. Introduction

Various drum-type machines remain basic equipment for the multi-tonnage processing of granular materials in many industrial sectors. This is predetermined by a number of operational and economic advantages of such equipment.

The utmost simplicity of the design of drum machines, however, is paradoxically combined with the behavior of the

treated medium that is extremely difficult to describe. The joint action of the gravitational and distorted centrifugal force fields results in the increased complexity of the flow of granular fill of a rotating chamber, which considerably complicates modeling of characteristics. The lack of a generally accepted technique for predicting the behavior of filling substantially limits effectiveness of the implementation of technological processes when using such equipment.

Performing the working processes of machines of the drum type is predetermined by the character of the flow mode of granular fill in the cross section of a rotating chamber. That is why establishing the regularities of change in the geometric and kinematic pattern of such a flow appears to be a rather relevant task.

2. Literature review and problem statement

Motion modes of granular fill of the rotating cylindrical chamber substantially affect the implementation of technological processes and energy efficiency of the drive in the machines of the drum type [1]. Modeling the hydrodynamics of such flow regimes is of interest when studying various rotor systems [2].

The applied relevance of the task on predicting workflows of this common technological equipment has been attracting increased research attention to describing the behavior of the treated granular medium. Significant complexity of the given problem calls for improvement in the traditional techniques, as well as necessitates application of the new theoretical and experimental research methods.

There have been many attempts aimed at solving numerically the problem on determining parameters of the flow patterns of granular fill in a rotating chamber.

A discrete elements method (DEM) was most often employed for numerical studies.

In paper [3], by using the DEM method, authors performed simulation of the motion patterns of filling the chamber that rotated at slow velocity with particles of lamellar form. While numerically studying the influence of roughness of the chamber walls on the flow regimes, based on the given method, authors of [4] determined motion patterns of granular fill in the chamber that rotates in a wide range of velocity's. They examined parameters of a series of flow modes – from crumbling to a centrifuge mode. The effect of change in the speed of rotation in a narrow low range, a degree of filling the chamber with wet particles and their adhesion, on the medium motion pattern was investigated in [5] applying the DEM method. Such a method was employed in [6] in order to determine the influence of roughness of the end walls of rotating chamber on the flow patterns of fill comprising the non-spherical particles, mainly of a cubic shape. A multiscale model was applied in the DEM method in [7] for determining the impact of the crushed material on the flow patterns of granular inside-the-chamber milling fill of the tumbling mills. In article [8], authors applied the DEM method for the systems of non-spherical particles in order to determine flow patterns of granular fill of the rotating chamber. Using graphics processors in the DEM method allowed authors in [9] to determine the influence of relative size of the particles on velocity distribution of flow patterns of the fill in a chamber that rotated at low velocity. In [10], the DEM method was exploited to study the impact of shape of non-spherical particles on velocity distribution of flow patterns of the fill in a chamber that slowly rotated. By using the DEM method, authors in [11] investigated the effect of shape of lamellar particles and roughness of the end walls of short chambers on the fill flow patterns. In [12], a model was employed of the built-in deformed solid spherical particles in line with the DEM method to study flow patterns inside a rotating chamber filled with polygonal particles. The authors considered influence of the shape of particles on the distribution of flow velocities. The DEM method was also applied in [13] in order to model flow patterns of a rotating chamber's fill consisting of ellipsoidal particles depending on the particle shape and rotation velocity. The authors investigated overfill modes, as well as the cataract flow of filling.

Several algorithms were proposed for determining numerically the flow patterns of granular fill in the rotating chamber based on the improved DEM method.

In paper [14], authors applied a new variant of the DEM method to study the flow patterns of a rotating chamber's fill consisting of convex non-spherical particles. A numerical Gilbert-Johnson-Keerthi algorithm was proposed for the simulation of flow of spherical, cylindrical, cubic, and tetrahedral particles. [15] describes using the DEM method developed for systems with arbitrary geometry and boundaries, which is based on the wide use of graphics processors. By applying such an algorithm, the authors obtained flow patterns of the fill consisting of ellipsoidal particles in the chamber that rotated at low velocity. The DEM method was complemented in [16] with a model of computational fluid dynamics in order to study interaction between non-spherical particles, in particular, for determining flow patterns of the fill in a rotating chamber. The authors substantiated prospects for further development of the given method.

A number of numerical algorithms were also developed, alternative to the DEM method, for the simulation of granular fill's flow in a rotating chamber.

In paper [17], authors employed a molecular dynamics algorithm to explore behavior and distribution of velocities of the active sliding layer and the solid-state zone of granular fill in a slow-rotating chamber. In [18], authors applied a finite element method in the Euler statement with the Mohr-Coulomb elastic model to identify flow patterns and velocity fields of granular fill in a rotating chamber. The authors investigated six motion modes in a wide range of change in the chamber's rotation velocity – from the offset to a centrifuge mode. The Euler's multiphase model of the method for computational fluid dynamics was applied in [19] in order to determine flow patterns of the chamber's fill depending on a change in the rotation velocity and the degree of filling. In [20], authors examined the use of a finite element method's large-scale model and its advantages in comparison with the DEM method, in order to determine the flow of granular fill in a slow-rotating chamber.

The initial conditions of the problem under consideration are, however, undefined in advance while the boundary conditions are of a non-physical nature. This imposes a significant constraint on the accuracy of numerical calculations whose results do not meet practical needs.

Flow patterns of granular fill in the rotating chamber were also investigated by experimental methods.

To determine geometrical and velocity characteristics of the flow, researchers mostly employed a method of visual analysis of flow patterns in the cross section of a chamber using video recording.

By applying a method of high-speed video recording, authors in [21] studied flow patterns of granular fill in the

cross-sectional and axial-sectional areas of a rotating chamber, depending on the velocity of rotation and relative size of the particles. Video recording with subsequent image processing was used in [22] in order to study flow patterns of the rotating chamber's fill consisting of lamellar particles, depending on a change in the velocity of rotation and the degree of filling. In [23], authors employed a high-speed video recording to determine flow patterns of the steel-ball fill of a rotating chamber.

The limited possibilities for visualization predetermined the application of tomographic methods to analyze behavior of granular fill of the rotating chamber. A particle tracking method was used in [24] in order to study flow patterns in the rotating chamber of granular fill with a quid dispersed phase. The authors examined the influence of change in the degree of filling the chamber, in the rotation speed, and in the viscosity of liquid phase, on the fill's flow modes.

At the same time, technical difficulties in the implementation of hardware control over behavior of the granular fill in a rotating chamber, due to the limited resolution capacity of the measuring equipment, reduce the reliability and accuracy of the results obtained in the course of experimental studies.

Given the limited possibilities of numerical and experimental methods, a comparison of the results of their application was conducted in determining geometrical and velocity characteristics of the flow patterns of granular fill in a rotating chamber.

In paper [25], authors compared results of research into flow patterns of the fill of a chamber under the modes of flow by overfill, cascade and cataract flow, which were obtained by the numerical method of DEM and by the experimental method of modeling using a soft sensor. Comparison of the results of computing applying the DEM method and by digital visualization of velocity distribution of flow patterns of the ball fill of a rotating chamber is given in [26]. In [27], authors investigated geometrical and velocity characteristics of flow patterns of granular fill of the rotating chamber, a wide range of variations of parameters of the system, which were obtained when applying the Euler's multiphase model of the DEM method and by running a visual analysis of data acquired from high-speed video recording. The results of determining a position of the free surface of flow patterns of mono- and two-dispersed granular fill in a slow-rotating chamber, which were obtained by using video recording and calculated by applying the DEM method, are given in [28]. In paper [29], authors compared results of research into flow patterns of the ball fill of a rotating chamber under cascade, cataract, and centrifuge modes, which were received by employing the method of computational fluid dynamics in the Euler's statement and visual analysis of video recording data. Similar methods of numerical and experimental studies were applied in [30]. The authors conducted a comparative assessment of modeling the flow patterns of granular material at a small fill of a slowly-rotating chamber with protruding elements on the surface.

Wide application of numerical and experimental methods, however, demonstrated limited possibilities of studies into behavior of the granular fill of a rotating chamber. Consequently, it appears advisable to bring in analytical methods that would make it possible to receive universal results with a high level of generalization. The use of such methods, however, is substantially complicated due to the characteristic features of the problem under consideration. This is related to the complexity of the geometry of the flow, a large deformation of the free boundary, dilatancy of the medium, and the mobility of a solid wall.

As a result, attempts at employing the analytical methods for determining a granular flow were limited to only one extremely simplified problem. It came down to modeling a two-phase mode of the fill flow [31] when a quasi-solid zone and a zone of tossing with falling form in the cross section of a chamber. Such an approach is based on the concept of a separate element of the chamber's fill, isolated from the surrounding medium, which moves only under the action of mass forces of gravity and centrifugal inertia, as well as the reaction of the bounding surface. According to this hypothesis, interaction between the elements is not taken into account. Due to extreme simplification, such a model allows simple and comprehensive formalization of the flow of idealized medium. The actual flow mode of granular fill in a rotating chamber, however, is three-phase, with the formation of active sliding layer near the free surface.

The difficulties in modeling the dynamic behavior of granular fill in a rotating chamber are complemented by rheological aspect. Paper [32] estimated the complexity and practical importance of determining adequately the rheological properties of granular media for the case of solving a problem on determining the fill's flow in a rotating chamber by applying an analytical method. It is indicated that the rheological characteristics of such environments significantly vary depending on the type of flow.

However, the insurmountable computational difficulties and low reliability of hardware control limit effectiveness of the known methods for determining geometrical and kinematic parameters of the chamber's granular fill flow. That is why the obtained results of numerical calculations and experiments approach actual flow modes of the examined medium only by qualitative characteristics and external features. In addition, they are relevant mainly to a slow-rotating chamber. Such data are substantially divergent in terms of quantitative indicators.

Given the above, at present, there are no created generalized analytical models of dynamic characteristics for the flow patterns of a rotating chamber's granular fill taking into account variations in a wide range of geometric and rheological parameters of the system. The lack of such models is particularly evident for the case of a non-low rotation velocity and the degree of filling the chamber.

3. The aim and objectives of the study

The aim of present work is to construct a mathematical model for the pattern of a steady flow of granular fill in the cross section of a cylindrical chamber that permanently rotates around a horizontal axis. This would make it possible to specify dynamic parameters of the fill flow and to predict effectiveness of the implementation of technological processes for processing granular medium in the rotating chamber.

To achieve the aim, the following tasks have been set:

– to perform an analytical-experimental modeling of the characteristics of a three-phase pattern of the flow mode of granular fill in the cross-sectional area of a rotating chamber;

– to identify position of the flow zones and velocity distribution in the fill flows;

– to establish conditions when the mass particles of the fill motion zones reach extreme values;

– to determine the conditions for changing and reaching extreme values of geometrical and kinematic parameters of non-free-falling zones and sliding layer of the fill;

– to clarify the influence of relative size of the element of a granular fill of the chamber on the geometrical and kinematic characteristics of the sliding layer.

4. Technique for studying behavior of the chamber's fill

4. 1. General conceptual approach to the research methodology

A granular fill of the rotating chamber was approximated with a multiphase polydispersed system. We employed a hypothesis on the continuity of the filling medium. The state of such a medium was described by characteristics averaged by volume, which are continuously distributed in space.

Rheological properties of the fill's granular media were formalized with a plastic model. It was assumed that resistance to displacement at the point of filling consisted of the resistance due to internal friction and adhesion, and is expressed by dependence that occurs when the equilibrium is broken.

$$|\tau_n| = \sigma_n \operatorname{tg}\varphi + k,$$

where σ_n and τ_n are the normal and tangent components of pressure, n is the normal to the sliding surface, φ is the angle of internal friction of the granular medium, k is the adhesion coefficient of the medium.

To determine the motion of the sliding layer at strict approach, we applied a system of equations (1)–(5) status of a two-dimensional state of the granular medium

$$F_x - \frac{g}{\gamma}\left(\frac{\partial \sigma_x}{\partial x} + \frac{\partial \tau_{xy}}{\partial y}\right) = \frac{\partial V_x}{\partial t} + V_x\frac{\partial V_x}{\partial x} + V_y\frac{\partial V_x}{\partial y}, \quad (1)$$

$$F_y - \frac{g}{\gamma}\left(\frac{\partial \sigma_y}{\partial y} + \frac{\partial \tau_{yx}}{\partial x}\right) = \frac{\partial V_y}{\partial t} + V_x\frac{\partial V_y}{\partial x} + V_y\frac{\partial V_y}{\partial y}, \quad (2)$$

$$\left(\sigma_x - \sigma_y\right)^2 + 4\tau_{xy}^2 = \left(\sigma_x + \sigma_y + 2k\cdot \operatorname{ctg}\varphi\right)^2 \sin^2\varphi, \quad (3)$$

$$\frac{\partial V_x}{\partial x} + \frac{\partial V_y}{\partial y} = 0, \quad (4)$$

$$\frac{2\tau_{xy}}{\sigma_x - \sigma_y} = \frac{\frac{1}{2}\left(\frac{V_y}{V_x} - \frac{V_x}{V_y}\right) \pm \operatorname{tg}\varphi}{1 \mp \frac{1}{2}\left(\frac{V_y}{V_x} - \frac{V_x}{V_y}\right)\operatorname{tg}\varphi}, \quad (5)$$

where σ_x, σ_y and $\tau_{xy} = \tau_{yx}$ are the components of stress tensor; V_x and V_y are two projections of the velocity vector; F_x and F_y are the projections of mass forces; x and y are the coordinates; γ is the volumetric weight of the medium; g is the gravitational acceleration.

The first two equations of system (1)–(5) are the equations of medium behavior. In a general case, they are the equations of a two-dimensional motion. At rest, when $V_x = 0$ and $V_y = 0$, (1) and (2) are the equations of equilibrium. The third equation of the system is a condition for boundary equilibrium. The fourth equation is the condition of medium continuity. The fifth equation expresses the condition for a match between the direction of maximum rate of shear deformation and one of the families of sliding lines (active family).

4. 2. Applied methods for modeling flow patterns of the fill in the cross section of a chamber

We adopted a three-phase scheme of the granular fill's steady flow in the cross section of a chamber that permanently rotated around its horizontal axis (Fig. 1). Flow pattern of the fill in the cross section of the chamber contains three regions. A passive quasi-solid-body flow occurs in region I without a relative displacement of the fill's elements and sliding along the surface of the chamber. A non-free fall takes place in region II. Region III corresponds to the active sliding layer.

We applied a method of calculating the stressed-deformed state in order to solve analytically two problems on the behavior of the fill of a rotating chamber (Fig. 1).

Paper [33] determined position of the border of transition between region I and II, based on the approximate solution of equilibrium equations of the granular medium (1)–(3). Such a boundary was considered the sliding line of flow pattern during transition of the fill's elements from circular to quasi-parabolic trajectories. Coordinates of such line *AB* (Fig. 2, 3) can be calculated from expressions:

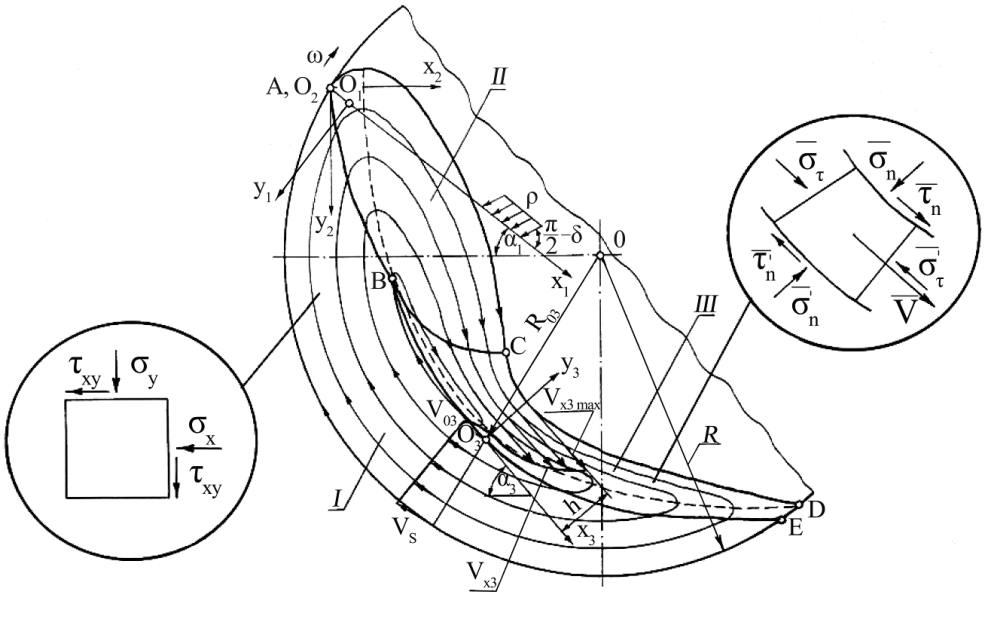

Fig. 1. General calculated schematic of flow pattern of the fill in the cross section of a rotating chamber

$$y_1 = b\sin(\alpha_1-\varphi)\frac{\sin 2\Omega}{\sin\alpha_1 \mp \sin\varphi\sin(2\Omega+\alpha_1)}, \quad (6)$$

$$x_1^{1,2} = \frac{2b\sin\alpha_1\sin(\alpha_1-\varphi)}{\sin^2\alpha_1-\sin^2\phi}\times$$
$$\times\left\{\frac{\left[\pm\cos\varphi(\mp\sin\varphi)-\sin\alpha_1\right]\cos(2\Omega+\alpha_1)}{2\left[\sin\alpha_1+(\mp\sin\varphi)\sin(2\Omega+\alpha_1)\right]}+\right.$$
$$+\frac{\pm\cos\varphi\sin\alpha_1-(\mp\sin\varphi)}{\sqrt{\sin^2\alpha_1-\sin^2\varphi}}\times$$
$$\times\operatorname{arctg}\left[\frac{\sin\alpha_1\cdot\operatorname{tg}\left(\Omega+\frac{\alpha_1}{2}\right)+(\mp\sin\varphi)}{\sqrt{\sin^2\alpha_1-\sin^2\varphi}}\right]-$$
$$-\frac{\left[\pm\cos\varphi(\mp\sin\varphi)-\sin\alpha_1\right]\cos\alpha_1}{2\left[\sin\alpha_1+(\mp\sin\varphi)\sin\alpha_1\right]}-$$
$$-\frac{\pm\cos\varphi\sin\alpha_1-(\mp\sin\varphi)}{\sqrt{\sin^2\alpha_1-\sin^2\varphi}}\times$$
$$\left.\times\operatorname{arctg}\left[\frac{\sin\alpha_1\cdot\operatorname{tg}\left(\frac{\alpha_1}{2}\right)+(\mp\sin\varphi)}{\sqrt{\sin^2\alpha_1-\sin^2\varphi}}\right]\right\}. \quad (7)$$

$$a = -\frac{p}{\gamma}\frac{\sin\delta}{\sin\alpha_1}, \quad (8)$$

$$b = \frac{p}{\gamma}\frac{\sin\varphi\sin(\alpha_1-\delta)}{\sin\alpha\sin(\alpha_1-\varphi)}, \quad (9)$$

$$p = \frac{\gamma\omega^2R^2}{2g}\left\{1-\left[\frac{\cos^2\beta}{\cos^2\left(\beta-\frac{\alpha_l}{2}\right)}\right]\right\}, \quad (10)$$

$$\alpha_1 = \alpha_l-\beta+\frac{\pi}{2}, \quad (11)$$

$$\delta = \frac{\alpha_l}{2}-\beta, \quad (12)$$

$$2\beta-\sin 2\beta = 2\pi\kappa. \quad (13)$$

Paper [34], based on the approximate solution to the flow equations of granular medium (1)–(5), determined velocity distribution along the normal to the direction of flow of the fill's sliding layer. A profile of shear velocity in the cross section of such layer (Fig. 1) can be determined from expressions:

$$V_{x3} = \sqrt{\left|2W\sin\alpha_3\frac{\cos\varphi}{1-\sin\varphi}y_3-V_{03}^2\right|}, \quad (14)$$

where $V_{x3}\le 0$ at

$$\left(2W\sin\alpha_3\frac{\cos\varphi}{1-\sin\varphi}y_3-V_{03}^2\right)\le 0$$

and

$$\left(2W\sin\alpha_3\frac{\cos\varphi}{1-\sin\varphi}y_3-V_{03}^2\right)\ge 0,$$

$$W = \sqrt[3]{-\frac{L}{2}+\sqrt{f}}+\sqrt[3]{-\frac{L}{2}-\sqrt{f}}-\frac{q}{3}, \quad (15)$$

$$f = \left(-\frac{q^2}{9}+\frac{m}{3}\right)^3+\left(\frac{L}{2}\right)^2, \quad (16)$$

$$L = 2\left(\frac{q}{3}\right)^3-\frac{qm}{3}-2\frac{V_{03}^6}{d^3}, \quad (17)$$

$$q = -\frac{1}{d^3}\left(\frac{V_{x3a}^2}{c^2}+3d^2V_{03}^2\right), \quad (18)$$

$$m = \frac{1}{d^3}\left(2\frac{V_{x3a}}{c}\left|V_{03}^3\right|+3dV_{03}^4\right), \quad (19)$$

$$V_{x3a} = \frac{\omega\left(R^2-R_{03}^2\right)}{2h}, \quad (20)$$

$$V_{03} = \omega R_{03}, \quad (21)$$

$$V_s = \omega R. \quad (22)$$

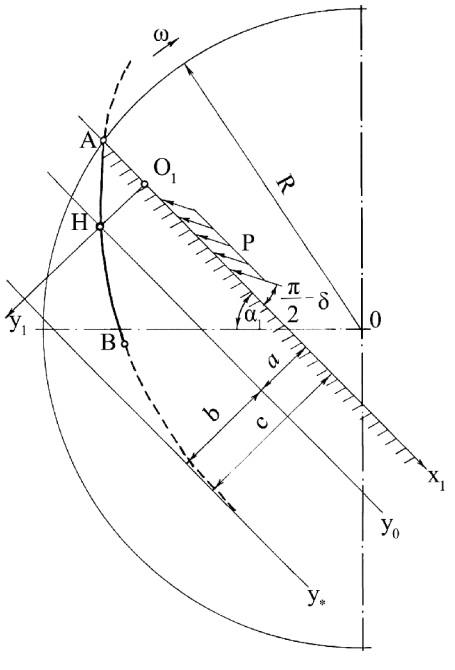

Fig. 2. Calculation scheme for the sliding line of the fill's flow pattern

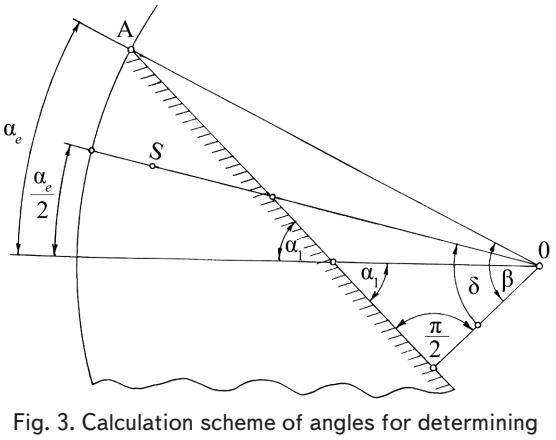

Fig. 3. Calculation scheme of angles for determining a sliding line of the fill's flow pattern

The method for calculating the stressed-deformed state of medium was supplemented with an analytical-experimental method of numerical studies into flow pattern of the fill in a rotating chamber. This method implied calculation of the position of the sliding surface and the velocity of the sliding layer and a quasi-solid-body region based on the obtained analytical dependences, with regard to the experimental data. Other geometrical characteristics of flow were determined based on the results of visual analysis of the recorded image of a flow pattern.

The algorithm for determining, using an analytical-experimental method, geometrical and kinematic parameters of the flow pattern of granular fill of a rotating chamber comprised the following stages (Fig. 1):

1. Assigning initial data for the formation of the fill's flow pattern:

– radius of chamber R;

– degree of filling the chamber with granular medium κ;

– specific weight of medium γ;

– angle of internal friction of medium φ;

– angular velocity of chamber rotation ω.

2. Obtaining experimentally a pattern of the fill's steady motion in the cross section of a permanently-rotating chamber.

3. Measurement of the magnitude of the fill's lifting angle in a rotating chamber α_l (Fig. 3), based on the experimental image of a flow pattern.

4. Construction, based on the calculated scheme of a flow pattern, employing the value of lifting angle α_l determined in point 3, of the position of point A (Fig. 3).

5. Determining from (13), by a consistent approximation, a half of the central angle of the segment cross section of the chamber's fill at rest β (Fig. 3).

6. Determining from (12) and (11):

– the tilt angle δ of the reduced pressure to the normal to the array's surface of the chamber's fill at rest;

– the tilt angle α_1 to the horizontal of free surface of the fill's array before sliding (Fig. 3).

7. Determining from (10) the reduced pressure on the fill's array surface p, which is due to the action of the applied centrifugal inertial forces on the central part of this array near point S (Fig. 3).

8. Determining from (9) and (8):

– width of the submerged band of fill b;

– width of the surface band of fill a (Fig. 2).

9. Determining from (6) and (7), by consistent approximation, coordinates of x_1 and y_1 of a section of the sliding line within the limits of the surface band of fill at $0 \le y_1 \le y_0$ ($0 \le y_1 \le a$) (Fig. 2). We adopt as a variable parameter the value of angle Ω between the direction of maximum stress σ_{max} and the x_1 axis. The calculation is performed for the respective active sliding line.

10. Construction, on the calculation scheme of a flow pattern, based on the coordinates defined in point 9, of a section of the sliding line within the limits of the surface band of fill above point H (Fig. 2) that passes through point A.

11. Determining from (6) and (7), by a consistent approximation, coordinates of x_1 and y_1 of the section of the sliding line within a submerged band of fill at $y_0 \le y_1 \le y_*$ ($a \le y_1 \le a+b$) (Fig. 2). We adopt as a variable parameter the value of angle Ω. The calculation is conducted for the opposite, in comparison with point 9, active sliding line.

12. Building on the calculation scheme of a flow pattern, based on the coordinates defined in point 9, a section of the sliding line within the limits of the submerged band of fill below point H (Fig. 2).

13. Construction on the calculation scheme of a flow pattern, considering its experimental mapping, near and below the intersection of the sliding line and the horizontal axial plane of the chamber (Fig. 2), of point B.

14. Building on the calculation scheme of a flow pattern, based on the experimental mapping of a flow pattern, of boundary BE between transition region of quasi-solid-body I and the region of non-free fall II.

15. Determining in the $0x_2y_2$ system of coordinates a free surface AC of the region of non-free fall II that approaches a parabolic dependence by its shape.

16. Building on the calculation scheme of a flow pattern, based on the coordinates defined in point 13, a free surface AC of the region of non-free fall II.

17. Construction on the calculation scheme of a flow pattern, based on the experimental mapping of motion pattern, of the boundary BC of the transition of the region of non-free fall II and the region of the sliding layer III and free surface CD of the region III.

18. Selection on the calculation scheme of a flow pattern of the position of the cross-section of the sliding layer of fill that is normal to the direction of flow on surface BE, and construction on BE of base 0_3 and the projection of this cross section that is perpendicular to BE at base 0_3.

19. Measurement on the experimental mapping of a flow pattern of the magnitude of radial coordinate of base R_{03}, thickness h, and inclination angle to the horizontal of supporting sliding surface α_3 of the normal cross-section of the fill's sliding layer.

20. Determining from (21) the flow velocity V_{03} of the base of normal cross-section of the sliding layer 0_3 that moves up along with the quasi-solid-body region I.

21. Determining from (20) the mean rate of the fill's flow in the normal cross section of layer V_{x3a}.

22. Determining from (19), (18), (17) and (16) variables m, q, L and f.

23. Determining from (15) conditional total vertical acceleration W, which predetermines kinematical parameters of motion in the normal cross section of the layer.

24. Selection on the calculation scheme of a flow pattern of the ordinates of points of the normal cross section of sliding layer y_3, including on the free surface of the layer at $y_{3max} = h$.

25. Determining from (14), for the points of normal cross section selected in point 19, the rates of flow of the sliding layer of fill V_{x3}, including V_{x3max} at $y_{3max} = h$.

26. Building on the calculation scheme of a flow pattern, based on the values obtained in point 20, of the profile of velocity distribution in the normal cross section of sliding layer $V_{x3}(y_3)$.

27. Determining from (22) the flow velocity of chamber surface V_s.

28. Construction on the calculation scheme of a flow pattern of the linear profile of velocity distribution, based on the values of V_{03} and V_s obtained in points 20–23 and 28. The profile is built in the radial cross section of a quasi-solid-body region of the fill below the base of the normal cross-section of sliding layer 0_3.

29. Selection, if required, on the calculation scheme of a motion pattern of the position of one or more other cross sections of the sliding layer of the fill that are normal to the direction of flow at surface BE.

30. Execution of points 18–28 for the normal cross sections of the fill's sliding layer, selected in point 29.

5. Results of simulation of the fill's flow pattern in the cross section of a chamber

Fig. 4–8 show the obtained calculation and experimental diagrams of the fill's flow patterns in the cross section of a rotating chamber for five flow modes.

The diagrams are shown in ascending order of acceleration in relative rotation velocity $\psi_\omega = \omega/\sqrt{g/R}$ and the degree of filling of the chambers κ.

The values of relative size of the fill's element $d/(2R)$, at average size d, ranged within 0.0024–0.026. We used a smooth and a wave cylindrical chamber surface.

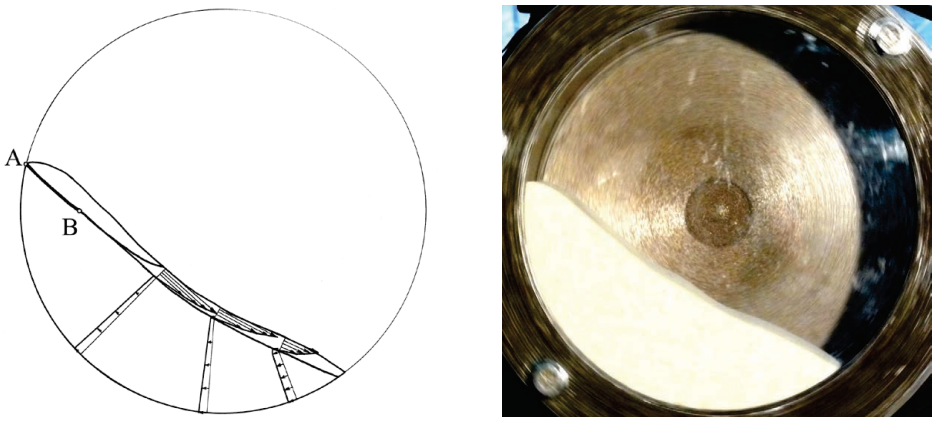

a *b*

Fig. 4. The fill's flow patterns at $\psi_\omega = 0.1$, $\kappa = 0.25$, $d/(2R) = 0.0024$ and smooth chamber surface: *a* — calculated; *b* — experimental

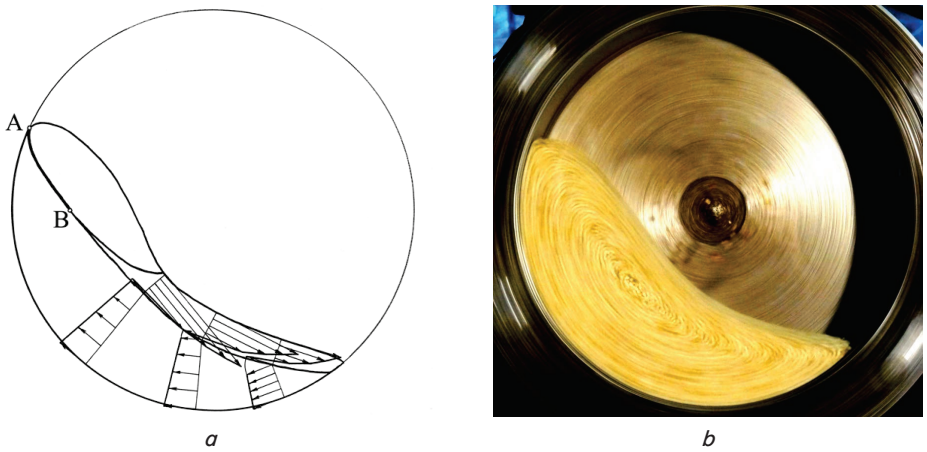

a *b*

Fig. 5. The fill's flow patterns at $\psi_\omega = 0.4$, $\kappa = 0.3$, $d/(2R) = 0.01$ and smooth chamber surface: *a* — calculated; *b* — experimental

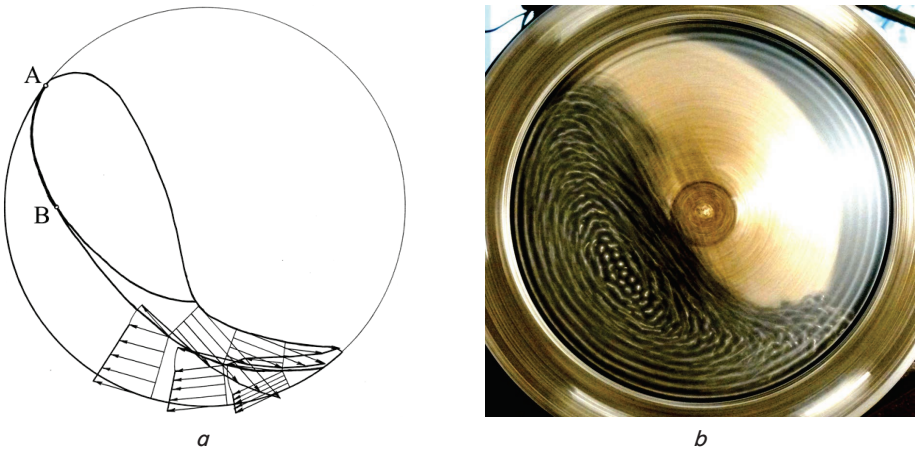

a *b*

Fig. 6. The fill's flow patterns at $\psi_\omega = 0.75$, $\kappa = 0.35$, $d/(2R) = 0.026$ and smooth chamber surface: *a* — calculated; *b* — experimental

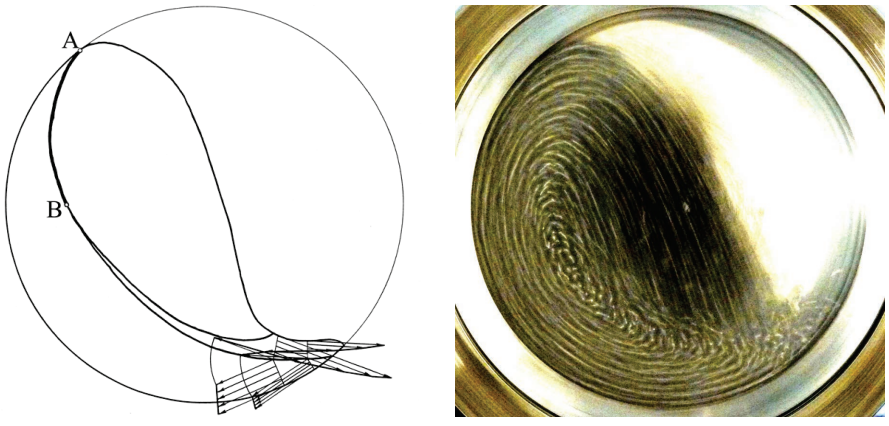

a *b*

Fig. 7. The fill's flow patterns at $\psi_\omega = 0.9$, $\kappa = 0.4$, $d/(2R) = 0.022$ and smooth chamber surface: *a* — calculated; *b* — experimental

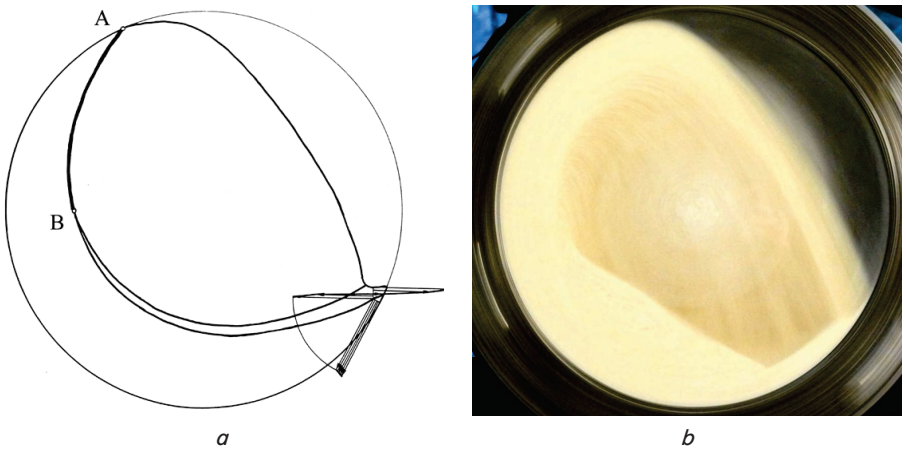

a *b*

Fig. 8. The fill's flow patterns at $\psi_\omega = 1.05$, $\kappa = 0.45$, $d/(2R) = 0.0024$ and smooth chamber surface: *a* — calculated; *b* — experimental

Previously, there was registered a manifestation of the effect of averaging the rheological parameters of granular materials at active circulating flow in the rotating chamber. Given this, the value of internal friction angle φ for all types of fill was taken the same and equal to about 33°.

The calculation diagrams of flow patterns show obtained sliding lines *AB* and the profiles of velocity in several cross sections of the sliding layer and corresponding radial cross sections of the quasi-solid-body region. The values of the constructed velocity profiles were executed comparable to the values of linear velocities of the chambers surfaces. For ease of comparison, the scale of velocity for all flow patterns was accepted to be the same.

We compared results of modeling the fill's flow patterns to experimental diagrams.

Fig. 9 shows the obtained calculation and experimental positions of the fill's sliding surface that correspond to the five flow patterns in Fig. 4, *a*–8, *a*.

Fig. 10 shows the obtained calculation and experimental profiles of the flow velocity in the top upper cross sections of the sliding layer that correspond to the five flow patterns in Fig. 4, *a*–8, *a*.

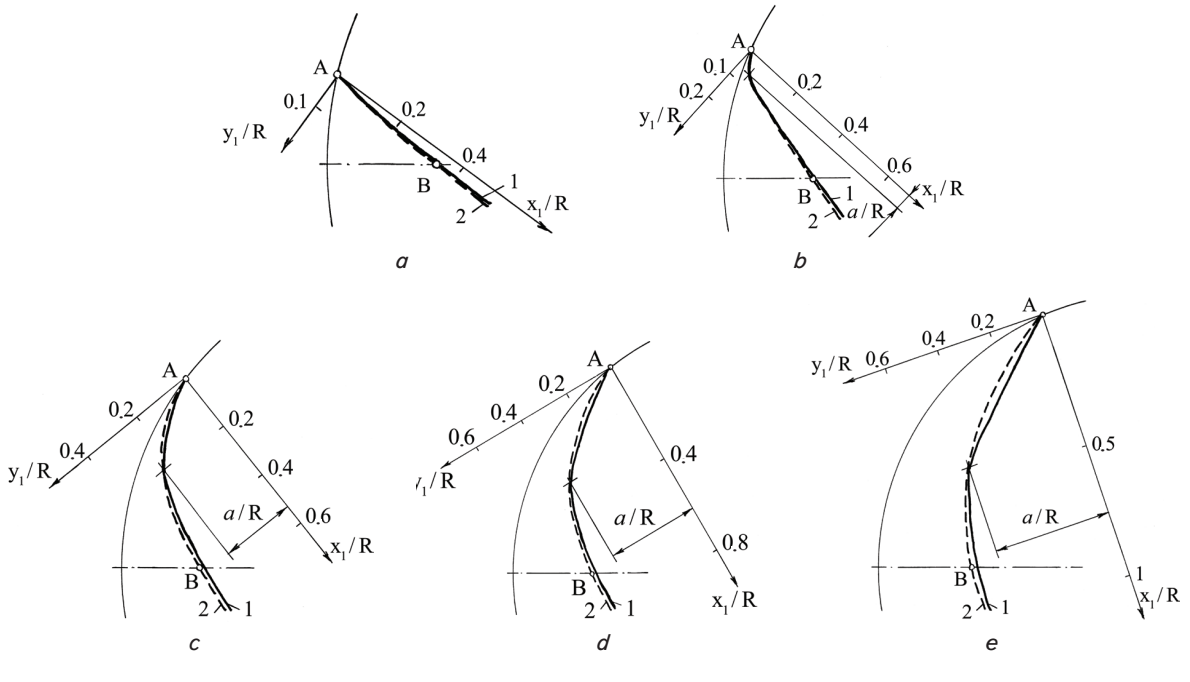

a *b* *c* *d* *e*

Fig. 9. Positions of the sliding surface that correspond to the flow patterns in Fig. 4, *a*—8, *a*: 1 — calculated surface; 2 — experimental surface; *a* — Fig. 4, *a*; *b* — Fig. 5, *a*; *c* — Fig. 6, *a*; *d* — Fig. 7, *a*; *e* — Fig. 8, *a*

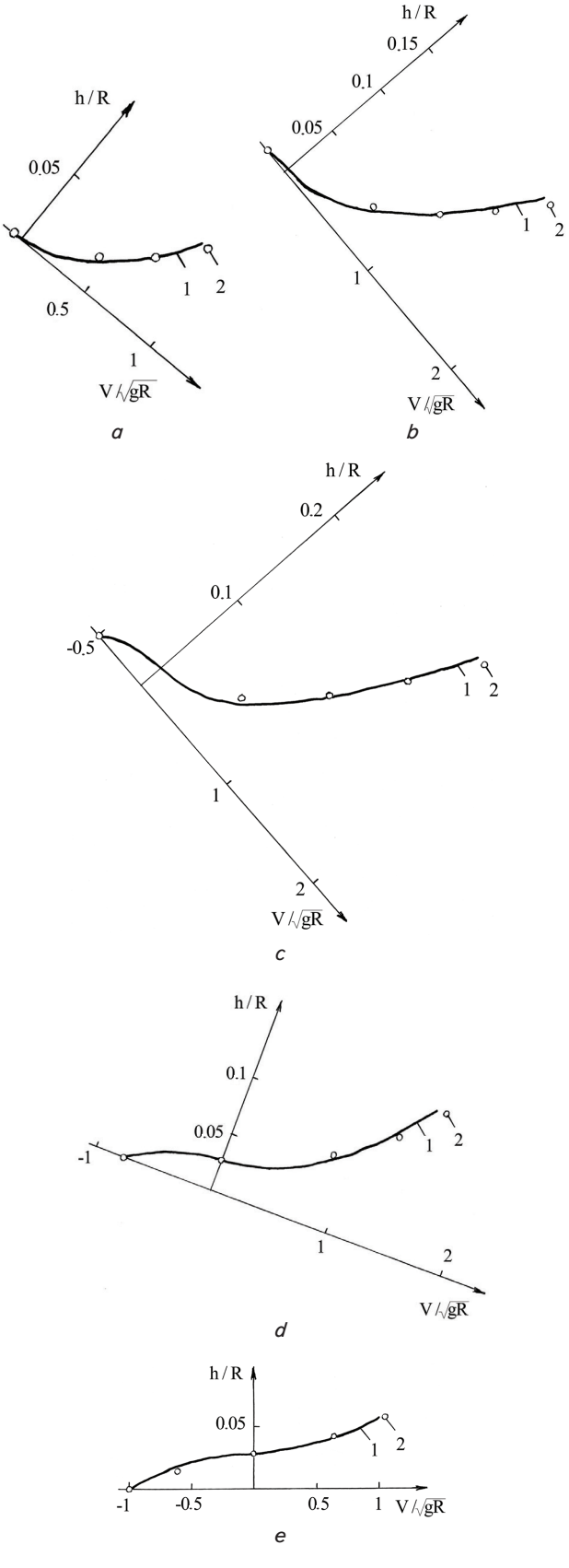

Fig. 10. Profiles of flow velocity in the upper cross sections of the sliding layer that correspond to the flow patterns in Fig. 4, *a*—8, *a*: 1 — calculated profile; 2 — experimental profile; *a* — Fig. 4, *a*; *b* — Fig. 5, *a*; *c* — Fig. 6, *a*; *d* — Fig. 7, *a*; *e* — Fig. 8, *a*

Results of the calculation of the sliding surface (Fig. 9) and the velocity profiles (Fig. 10) are close to the experimental data.

6. Discussion of results of studying the influence of parameters of the filled rotating chamber on the fill's flow patterns

Description of the flow pattern of granular fill in a rotating chamber is based on the analytical-experimental method. Mathematical notation of the flow pattern was performed analytically in line with the classical scheme using the magnitudes averaged by volume. The initial and boundary conditions, required for solving the equations obtained, were determined experimentally employing a method for the visualization of flow patterns. Such a calculation algorithm made it possible to establish approximately the dependences of characteristics of the flow patterns on a number of parameters of the examined system:

– geometrical: chamber radius R, radial coordinate of the base of normal cross-section of sliding layer R_{03}, thickness of this layer h and the degree of filling the chambers κ;

– kinematic: angular velocity of chamber rotation ω;

– inertial: specific bulk weight of fill γ;

– rheological: angle of internal friction of the fill φ, lifting angel of the fill in a rotating chamber α_l and inclination angle of the supporting surface of sliding layer to the horizontal α_3.

The advantage of the proposed approach is the possibility for determining quantitative geometrical and kinematic characteristics of flow pattern – a position of the regions of flow and the fields of filling rate. In addition, compared with the traditional hypothesis [31], it is possible to determine flow patterns depending on the values of parameters R, R_{03}, h, κ, ω, γ, φ, α_l and α_3. More to the point, the traditional model of a two-phase motion mode of granular fill of the rotating chamber does not imply the occurrence and modeling of the sliding layer flow.

An analysis of Fig. 4–8 confirms that the mass fraction of the region of active sliding layer of the filled chamber acquires a maximum at the value of relative rotation velocity of $\psi_\omega \approx 0.1$–0.4. In this case, the mass fraction of the region of a non-free fall reaches a maximum, while the mass fraction of the passive quasi-solid-body region acquires a minimum, at $\psi_\omega \approx 0.9$–1.05.

A comparative analysis reveals good convergence of the characteristics of the fill's flow patterns, obtained by calculation and by experimental method. The discrepancy between results of determining a position of the sliding surface for the five flow patterns (Fig. 9) does not exceed 13 %. The discrepancy between results of determining a velocity profile of the sliding layer (Fig. 10) does not exceed 11 %.

Thickness of the sliding layer has the maximum value at $\psi_\omega \approx 0.75$. The length of such a layer decreases with increasing rotation velocity. The average flow velocity of the sliding layer reaches a maximum at $\psi_\omega \approx 0.75$–0.9.

A decrease in the dynamic activity along the length of the sliding layer occurs in the direction of flow. It manifests itself in the prevailing reduction of the values of thickness, mean velocity and a gradient of shear velocity in the normal cross section of the layer.

With a decrease in the relative size of the fill's element $d/(2R)$, a thickness of the sliding layer is reduced, while the mean flow velocity and the gradient of shear speed increase.

The height of fall of the region of a non-free fall reaches a maximum at $\psi_\omega \approx 0.9–1.05$.

The shortcomings of the developed algorithm for numerical calculation of the flow pattern include the need for a preliminary experimental determination of a number of geometrical parameters of the fill flow by using a method of visualization. These parameters are the lifting angle of the fill in a rotating chamber α_l, radial coordinate of the base of selected normal cross section of the sliding layer R_{03}, thickness h, and the inclination angle α_3 of the layer to the horizontal in this cross section and boundaries of regions *CD*, *BE*, and *BC*. In addition, the applied algorithm makes it possible to clarify only qualitatively the patterns of manifestation of a three-phase regime of the fill's flow and does not allow performing a quantitative analysis of the flow's dynamic characteristics that define technological efficiency of the drum machines.

In the future, it is advisable to choose criteria of efficiency for the implementation of workflows to process granular fill in a rotating chamber, which are predetermined by the mode of medium flow, and to establish values of the fill's flow patterns by using the analytical-experimental method of calculation, applied in the present work. It appears appropriate to determine the quantitative dependences of such criteria on the variation of system's parameters, including the degree of filling the chamber κ and the relative size of fill's elements $d/(2R)$. This will make it possible to establish rational technological parameters for machines of the drum type.

7. Conclusions

1. We formalized flow patterns of the fill in the cross-section of a rotating chamber by using the analytical-experimental method for determining a two-dimensional state of movable granular medium. It was found that characteristics of the fill's flow patterns depend on the magnitude of angular velocity of chamber rotation ω, chamber radius R, a degree of filling the chamber κ, specific bulk weight of granular fill γ, angle of the fill's internal friction φ, the fill's lifting angle in a rotating chamber α_l, radial coordinate of the base of normal cross section of the sliding layer R_{03}, inclination angle to the horizontal of the base of cross section of layer α_3 and thickness of the cross section of layer h.

2. By employing the obtained calculation algorithm, we approximately determined position of the three regions of flow and the distribution of velocities in cross sections normal to the directions of flows, depending on the velocity of rotation, geometrical, inertial, and rheological parameters of the system.

3. The maximum value of mass fraction of the region of active sliding layer roughly corresponds to the range of the magnitude of relative rotation velocity of the chamber $\psi_\omega \approx 0.1–0.4$. The maximum value of mass fraction of the region of a non-free fall and the minimum value of mass fraction of the passive quasi-solid-body region roughly match the range of relative velocity $\psi_\omega \approx 0.9–1.05$.

4. The maximum value of thickness of the sliding layer of the fill roughly corresponds to the magnitude of relative velocity of rotation $\psi_\omega \approx 0.75$. The length of such a layer is reduced with increasing velocity. The maximum value of the mean flow velocity of the sliding layer roughly corresponds to the range of relative velocity $\psi_\omega \approx 0.75–0.9$. Thickness, mean velocity and the gradient of shear velocity in the normal cross section of the fill's sliding layer are mostly reduced along its length in the direction of flow.

5. Thickness of the sliding layer is reduced, while its average velocity and the gradient of shear rate increases, with a decrease in the relative size of the granular fill's element of a chamber.

References

1. Naumenko, Yu. V. The antitorque moment in a partially filled horizontal cylinder [Text] / Yu. V. Naumenko // Theoretical Foundations of Chemical Engineering. – 1999. – Vol. 33, Issue 1. – P. 91–95.
2. Naumenko, Yu. V. Determination of rational rotation speeds of horizontal drum machines [Text] / Yu. V. Naumenko // Metallurgical and Mining Industry. – 2000. – Issue 5. – P. 89–92.
3. Liu, X. Granular flow in a rotating drum with gaps in the side wall [Text] / X. Liu, W. Ge, Y. Xiao, J. Li // Powder Technology. – 2008. – Vol. 182, Issue 2. – P. 241–249. doi: 10.1016/j.powtec.2007.06.029
4. Yang, R. Y. Numerical simulation of particle dynamics in different flow regimes in a rotating drum [Text] / R. Y. Yang, A. B. Yu, L. McElroy, J. Bao // Powder Technology. – 2008. – Vol. 188, Issue 2. – P. 170–177. doi: 10.1016/j.powtec.2008.04.081
5. Liu, P. Y. DEM study of the transverse mixing of wet particles in rotating drums [Text] / P. Y. Liu, R. Y. Yang, A. B. Yu // Chemical Engineering Science. – 2013. – Vol. 86. – P. 99–107. doi: 10.1016/j.ces.2012.06.015
6. Lu, G. Effect of wall rougheners on cross-sectional flow characteristics for non-spherical particles in a horizontal rotating cylinder [Text] / G. Lu, J. R. Third, C. R. Müller // Particuology. – 2014. – Vol. 12. – P. 44–53. doi: 10.1016/j.partic.2013.03.003
7. Cleary, P. W. A multiscale method for including fine particle effects in DEM models of grinding mills [Text] / P. W. Cleary // Minerals Engineering. – 2015. – Vol. 84. – P. 88–99. doi: 10.1016/j.mineng.2015.10.008
8. Lu, G. Discrete element models for non-spherical particle systems: From theoretical developments to applications [Text] / G. Lu, J. R. Third, C. R. Müller // Chemical Engineering Science. – 2015. – Vol. 127. – P. 425–465. doi: 10.1016/j.ces.2014.11.050
9. Qi, H. Numerical investigation of granular flow similarity in rotating drums [Text] / H. Qi, J. Xu, G. Zhou, F. Chen, W. Ge, J. Li // Particuology. – 2015. – Vol. 22. – P. 119–127. doi: 10.1016/j.partic.2014.10.012
10. Norouzi, H. R. Insights into the granular flow in rotating drums [Text] / H. R. Norouzi, R. Zarghami, N. Mostoufi // Chemical Engineering Research and Design. – 2015. – Vol. 102. – P. 12–15. doi: 10.1016/j.cherd.2015.06.010
11. Zhang, Z. Numerical study of mixing of binary-sized particles in rotating tumblers on the effects of end-walls and size ratios [Text] / Z. Zhang, N. Gui, L. Ge, Z. Li // Powder Technology. – 2017. – Vol. 314. – P. 164–174. doi: 10.1016/j.powtec.2016.09.072
12. Gui, N. Numerical simulation and analysis of mixing of polygonal particles in 2D rotating drums by SIPHPM method [Text] / N. Gui, X. Yang, J. Tu, S. Jiang // Powder Technology. – 2017. – Vol. 318. – P. 248–262. doi: 10.1016/j.powtec.2017.06.007

13. Ma, H. Modelling of the flow of ellipsoidal particles in a horizontal rotating drum based on DEM simulation [Text] / H. Ma, Y. Zhao // Chemical Engineering Science. – 2017. – Vol. 172. – P. 636–651. doi: 10.1016/j.ces.2017.07.017
14. Wachs, A. Grains3D, a flexible DEM approach for particles of arbitrary convex shape – Part I: Numerical model and validations [Text] / A. Wachs, L. Girolami, G. Vinay, G. Ferrer // Powder Technology. – 2012. – Vol. 224. – P. 374–389. doi: 10.1016/j.powtec.2012.03.023
15. Gan, J. Q. A GPU-based DEM approach for modelling of particulate systems [Text] / J. Q. Gan, Z. Y. Zhou, A. B. Yu // Powder Technology. – 2016. – Vol. 301. – P. 1172–1182. doi: 10.1016/j.powtec.2016.07.072
16. Zhong, W. DEM/CFD-DEM Modelling of Non-spherical Particulate Systems: Theoretical Developments and Applications [Text] / W. Zhong, A. Yu, X. Liu, Z. Tong, H. Zhang // Powder Technology. – 2016. – Vol. 302. – P. 108–152. doi: 10.1016/j.powtec.2016.07.010
17. Li, S. Molecular dynamics simulation and continuum modelling of granular surface flow in rotating drums [Text] / S. Li, Q. Yao, B. Chen, X. Zhang, Y. L. Ding // Chinese Science Bulletin. – 2007. – Vol. 52, Issue 5. – P. 692–700. doi: 10.1007/s11434-007-0069-4
18. Zheng, Q. J. Modelling the granular flow in a rotating drum by the Eulerian finite element method [Text] / Q. J. Zheng, A. B. Yu // Powder Technology. – 2015. – Vol. 286. – P. 361–370. doi: 10.1016/j.powtec.2015.08.025
19. Delele, M. A. Studying the solids and fluid flow behavior in rotary drums based on a multiphase CFD model [Text] / M. A. Delele, F. Weigler, G. Franke, J. Mellmann // Powder Technology. – 2016. – Vol. 292. – P. 260–271. doi: 10.1016/j.powtec.2016.01.026
20. Liu, Y. Modeling granular material blending in a rotating drum using a finite element method and advection-diffusion equation multi-scale model [Text] / Y. Liu, M. Gonzalez, C. Wassgren // Arxiv.org. – 2017. – Available at: https://arxiv.org/ftp/arxiv/papers/1704/1704.01219.pdf
21. Chou, H.-T. Cross-sectional and axial flow characteristics of dry granular material in rotating drums [Text] / H.-T. Chou, C.-F. Lee // Granular Matter. – 2008. – Vol. 11, Issue 1. – P. 13–32. doi: 10.1007/s10035-008-0118-y
22. Liu, X. Y. Experimental Study on Time Features of Particle Motion in Rotating Drums [Text] / X. Y. Liu, X. Xu, Y. Y. Zhang // Chemical Engineering & Technology. – 2011. – Vol. 34, Issue 6. – P. 997–1002. doi: 10.1002/ceat.201000483
23. Machado, M. V. C. Experimental Study of Charge Motion in a Tumbling Ball Mill [Text] / M. V. C. Machado, V. Straatmann, C. R. Duarte, M. A. de Souza Barrozo // Materials Science Forum. – 2017. – Vol. 899. – P. 119–123. doi: 10.4028/www.scientific.net/msf.899.119
24. Chou, S. H. Dynamic properties of immersed granular matter in different flow regimes in a rotating drum [Text] / S. H. Chou, S. S. Hsiau // Powder Technology. – 2012. – Vol. 226. – P. 99–106. doi: 10.1016/j.powtec.2012.04.024
25. McElroy, L. A soft-sensor approach to flow regime detection for milling processes [Text] / L. McElroy, J. Bao, R. Y. Yang, A. B. Yu // Powder Technology. – 2009. – Vol. 188, Issue 3. – P. 234–241. doi: 10.1016/j.powtec.2008.05.002
26. Pérez-Alonso, C. Experimental validation of 2D DEM code by digital image analysis in tumbling mills [Text] / C. Pérez-Alonso, J. A. Delgadillo // Minerals Engineering. – 2012. – Vol. 25, Issue 1. – P. 20–27. doi: 10.1016/j.mineng.2011.09.018
27. Santos, D. A. Experimental and CFD study of the hydrodynamic behavior in a rotating drum [Text] / D. A. Santos, I. J. Petri, C. R. Duarte, M. A. S. Barrozo // Powder Technology. – 2013. – Vol. 250. – P. 52–62. doi: 10.1016/j.powtec.2013.10.003
28. Cunha, R. N. Repose angle of monoparticles and binary mixture: An experimental and simulation study [Text] / R. N. Cunha, K. G. Santos, R. N. Lima, C. R. Duarte, M. A. S. Barrozo // Powder Technology. – 2016. – Vol. 303. – P. 203–211. doi: 10.1016/j.powtec.2016.09.023
29. Machado, M. V. C. Experimental and Numerical Study of Grinding Media Flow in a Ball Mill [Text] / M. V. C. Machado, D. A. Santos, M. A. S. Barrozo, C. R. Duarte // Chemical Engineering & Technology. – 2017. doi: 10.1002/ceat.201600508
30. Nascimento, S. M. Numerical Simulation and Experimental Study of Particle Dynamics in a Rotating Drum with Flights [Text] / S. M. Nascimento, F. P. de Lima, C. R. Duarte, M. A. de Souza Barrozo // Materials Science Forum. – 2017. – Vol. 899. – P. 65–70. doi: 10.4028/www.scientific.net/msf.899.65
31. Andreev, S. E. Droblenie, izmel'chenie i grohochenie poleznyh iskopaemyh [Text] / S. E. Andreev, V. A. Perov, V. V. Zverevich. – Moscow: Nedra, 1980. – 415 p.
32. Govender, I. Granular flows in rotating drums: A rheological perspective [Text] / I. Govender // Minerals Engineering. – 2016. – Vol. 92. – P. 168–175. doi: 10.1016/j.mineng.2016.03.021
33. Naumenko, Y. Modeling of fracture surface of the quasi solid-body zone of motion of the granular fill in a rotating chamber [Text] / Y. Naumenko // Eastern-European Journal of Enterprise Technologies. – 2017. – Vol. 2, Issue 1 (86). – P. 50–57. doi: 10.15587/1729-4061.2017.96447
34. Naumenko, Y. The rotating chamber granular fill shear layer flow simulation [Text] / Y. Naumenko, V. Sivko // Eastern-European Journal of Enterprise Technologies. – 2017. – Vol. 4, Issue 7 (88). – P. 57–64. doi: 10.15587/1729-4061.2017.107242